Biomedical Optics EXPRESS

A hybrid silicon-PDMS optofluidic platform for sensing applications

Genni Testa,[1,*] Gianluca Persichetti,[1] Pasqualina M. Sarro,[2] and Romeo Bernini[1]

[1]*Institute for Electromagnetic Sensing of the Environment (IREA), National Research Council, (CNR), Via Diocleziano 328, 80124 Napoli, Italy*

[2]*DIMES-ECTM, Delft University of Technology, Feldmannweg 17, 2628 CT Delft, The Netherlands*

[*]*testa.g@irea.cnr.it*

Abstract: A hybrid silicon-poly(dimethysiloxane) (PDMS) optofluidic platform for lab-on-a-chip applications is proposed. A liquid-core waveguide with a self-aligned solid-core waveguide and a microfluidic device are integrated with a multilayer approach, resulting in a three-dimensional device assembly. The optofluidic layer was fabricated with a hybrid silicon-polymer technology, whereas the microfluidic layer was fabricated with a soft lithography technique. The combination of different materials and fabrication processes allows a modular approach, enabling both the benefits from the high optical quality achievable with silicon technology and the low cost of polymer processing. The proposed chip has been tested for fluorescence measurements on Cy5 water solutions, demonstrating the possibility to obtain a limit of detection of 2.5 nM.

OCIS codes: (130.0130) Integrated optics; (130.3990) Micro-optical devices; (280.4788) Optical sensing and sensors.

References and links

1. B. Kuswandi, Nuriman, J. Huskens, and W. Verboom, "Optical sensing systems for microfluidic devices: a review," Anal. Chim. Acta **601**(2), 141–155 (2007).
2. K. B. Mogensen and J. P. Kutter, "Optical detection in microfluidic systems," Electrophoresis **30**(S1 Suppl 1), S92–S100 (2009).
3. F. B. Myers and L. P. Lee, "Innovations in optical microfluidic technologies for point-of-care diagnostics," Lab Chip **8**(12), 2015–2031 (2008).
4. A. Schaap, Y. Bellouard, and T. Rohrlack, "Optofluidic lab-on-a-chip for rapid algae population screening," Biomed. Opt. Express **2**(3), 658–664 (2011).
5. L. Zhu, C. S. Lee, and D. L. DeVoe, "Integrated microfluidic UV absorbance detector with attomol-level sensitivity for BSA," Lab Chip **6**(1), 115–120 (2006).
6. B. R. Watts, Z. Zhang, C.-Q. Xu, X. Cao, and M. Lin, "Integration of optical components on-chip for scattering and fluorescence detection in an optofluidic device," Biomed. Opt. Express **3**(11), 2784–2793 (2012).
7. K. S. Lee, H. L. T. Lee, and R. J. Ram, "Polymer waveguide backplanes for optical sensor interfaces in microfluidics," Lab Chip **7**(11), 1539–1545 (2007).
8. Y. Zhao, K. D. Leake, P. Measor, M. H. Jenkins, J. Keeley, H. Schmidt, and A. R. Hawkins, "Optimization of interface transmission between integrated solid core and optofluidic waveguides," IEEE Photon. Technol. Lett. **24**, 46–48 (2012).
9. O. Hofmann, X. Wang, A. Cornwell, S. Beecher, A. Raja, D. D. C. Bradley, A. J. Demello, and J. C. Demello, "Monolithically integrated dye-doped PDMS long-pass filters for disposable on-chip fluorescence detection," Lab Chip **6**(8), 981–987 (2006).
10. M. Fleger and A. Neyer, "PDMS microfluidic chip with integrated waveguides for optical detection," Microelectron. Eng. **83**(4-9), 1291–1293 (2006).
11. K. B. Mogensen, J. El-Ali, A. Wolff, and J. P. Kutter, "Integration of polymer waveguides for optical detection in microfabricated chemical analysis systems," Appl. Opt. **42**(19), 4072–4079 (2003).
12. C. Dongre, J. van Weerd, N. Bellini, R. Osellame, G. Cerullo, R. van Weeghel, H. J. W. M. Hoekstra, and M. Pollnau, "Dual-point dual-wavelength fluorescence monitoring of DNA separation in a lab on a chip," Biomed. Opt. Express **1**(2), 729–735 (2010).
13. R. M. Vazquez, R. Osellame, D. Nolli, C. Dongre, H. van den Vlekkert, R. Ramponi, M. Pollnau, and G. Cerullo, "Integration of femtosecond laser written optical waveguides in a lab-on-chip," Lab Chip **9**(1), 91–96 (2009).
14. D. Yin, J. P. Barber, A. R. Hawkins, and H. Schmidt, "Highly efficient fluorescence detection in picoliter volume liquid-core waveguides," Appl. Phys. Lett. **87**(21), 211111 (2005).

#194578 - $15.00 USD Received 24 Jul 2013; revised 9 Sep 2013; accepted 9 Oct 2013; published 9 Jan 2014

15. G. Persichetti, G. Testa, and R. Bernini, "Optofluidic jet waveguide for laser-induced fluorescence spectroscopy," Opt. Lett. **37**(24), 5115–5117 (2012).
16. H. Schmidt and A. R. Hawkins, "Optofluidic waveguides: I. Concepts and implementations," Microfluid Nanofluidics **4**(1-2), 3–16 (2008).
17. D. Yin, E. J. Lunt, M. I. Rudenko, D. W. Deamer, A. R. Hawkins, and H. Schmidt, "Planar optofluidic chip for single particle detection, manipulation, and analysis," Lab Chip **7**(9), 1171–1175 (2007).
18. P. Friis, K. Hoppe, O. Leistiko, K. B. Mogensen, J. Hübner, and J. P. Kutter, "Monolithic integration of microfluidic channels and optical waveguides in silica on silicon," Appl. Opt. **40**(34), 6246–6251 (2001).
19. H. Andersson and A. van den Berg, "Microfluidic devices for cellomics: a review," Sens. Actuators B Chem. **92**(3), 315–325 (2003).
20. L. Zhu, C. S. Lee, and D. L. DeVoe, "Integrated microfluidic UV absorbance detector with attomol-level sensitivity for BSA," Lab Chip **6**(1), 115–120 (2006).
21. A. Nitkowski, A. Baeumner, and M. Lipson, "On-chip spectrophotometry for bioanalysis using microring resonators," Biomed. Opt. Express **2**(2), 271–277 (2011).
22. K. Kalkandjiev, L. Riegger, D. Kosse, M. Welsche, L. Gutzweiler, R. Zengerle, and P. Koltay, "Microfluidics in silicon/polymer technology as a cost-efficient alternative to silicon/glass," J. Micromech. Microeng. **21**(2), 025008 (2011).
23. K. Kalkandjiev, R. Zengerle, and P. Koltay, "Hybrid fabrication of microfluidic chips based on COC, silicon and TMMF dry resist," in Proceedings of IEEE Conference on Micro Electro Mechanical Systems (MEMS) (IEEE, 2010), pp. 400–403.
24. J. M. K. Ng, I. Gitlin, A. D. Stroock, and G. M. Whitesides, "Components for integrated poly(dimethylsiloxane) microfluidic systems," Electrophoresis **23**(20), 3461–3473 (2002).
25. G. Testa, Y. Huang, L. Zeni, P. M. Sarro, and R. Bernini, "Hybrid Silicon-PDMS optofluidic ARROW waveguide," IEEE Photon. Technol. Lett. **24**(15), 1307–1309 (2012).
26. J. W. Parks, H. Cai, L. Zempoaltecatl, T. D. Yuzvinsky, K. Leake, A. R. Hawkins, and H. Schmidt, "Hybrid optofluidic integration," Lab Chip, Advanced (2013).
27. G. Testa, Y. Huang, L. Zeni, P. M. Sarro, and R. Bernini, "Liquid core ARROW waveguides by atomic layer deposition," IEEE Photon. Technol. Lett. **22**(9), 616–618 (2010).
28. G. Testa, Y. Huang, P. M. Sarro, L. Zeni, and R. Bernini, "Integrated silicon optofluidic ring resonator," Appl. Phys. Lett. **97**(13), 131110 (2010).
29. G. Testa, Y. Huang, P. M. Sarro, L. Zeni, and R. Bernini, "High-visibility optofluidic Mach-Zehnder interferometer," Opt. Lett. **35**(10), 1584–1586 (2010).
30. R. Bernini, S. Campopiano, L. Zeni, and P. M. Sarro, "ARROW optical waveguides based sensors," Sens. Actuators B Chem. **100**(1-2), 143–146 (2004).
31. T. M. Squires and S. R. Quake, "Microfluidics: Fluid physics at the nanoliter scale," Rev. Mod. Phys. **77**(3), 977–1026 (2005).
32. J. Wang, M. Zheng, W. Wang, and Z. Li, "Optimal protocol for moulding PDMS with a PDMS master," Chips & Tips (Lab on a Chip), 06 Jul 2010.
33. A. Pais, A. Banerjee, D. Klotzkin, and I. Papautsky, "High-sensitivity, disposable lab-on-a-chip with thin-film organic electronics for fluorescence detection," Lab Chip **8**(5), 794–800 (2008).
34. F. B. Myers and L. P. Lee, "Innovations in optical microfluidic technologies for point-of-care diagnostics," Lab Chip **8**(12), 2015–2031 (2008).
35. K. Miyaki, Y. Guo, T. Shimosaka, T. Nakagama, H. Nakajima, and K. Uchiyama, "Fabrication of an integrated PDMS microchip incorporating an LED-induced fluorescence device," Anal. Bioanal. Chem. **382**(3), 810–816 (2005).
36. R. Irawan, C. M. Tay, S. C. Tjin, and C. Y. Fu, "Compact fluorescence detection using in-fiber microchannels-its potential for lab-on-a-chip applications," Lab Chip **6**(8), 1095–1098 (2006).

1. Introduction

In recent years great effort has been devoted to the development of lab-on-a-chip (LOC) systems for health care and biosensing applications. In particular, optical detection methods, including absorbance and fluorescence, have been widely used [1–4]. However, although optical detection is commonly regarded as superior, its application in an LOC system is not an easy task. The integration of optical and optoelectronic components with microfluidics has been widely demonstrated to improve the overall performance of the devices [5,6]. For detection, a precise alignment of waveguides and microfluidic channels is required to probe very small volumes of analyte with high accuracy. Monolithic integration of micro-channels and optical waveguides has been used to improve sensitivity, providing a high level of integration and avoiding optical-fiber alignment problems [7–13]. Optofluidic waveguides are a highly promising alternative to conventional solid-core waveguides for high-sensitivity detection [14–16]. These waveguides are very compact tools, as the probing light propagates

#194578 - $15.00 USD Received 24 Jul 2013; revised 9 Sep 2013; accepted 9 Oct 2013; published 9 Jan 2014

along the same micro-channel wherein the liquid sample flows. However, even if this approach strongly improves the optical interaction of the probing light and the sensing volume, it does not solve the problem of integration of solid-core with liquid-core waveguides and the question related to the efficient light coupling with off-chip detection systems. Examples of LOCs fabricated by using silicon technology, where integration of optical waveguides and microfluidic channels has been successfully achieved, are worth mentioning [17].

Despite the significant technological advances in the development of compact, inexpensive, and high-sensitivity LOC microsystems, nowadays the full integration of microfluidic and micro-optic elements on the same platform is a major technical challenge. Several materials and fabrication technologies have been used for the realization of optical LOC systems [9–11,13,18]. Integrated silicon technologies have been demonstrated as a powerful tool that is able to achieve a high level of integration of optical structures and complex networks of microfluidic channels [17–19]. However, silicon technology processes require legacy capital equipment from the semiconductor industry, typically housed in a cleanroom that is extremely costly to run. Therefore, the use of silicon to fabricate some microfluidic devices such as reservoir, mixer, and fluid inlet and outlet is costly and time consuming. In order to overcome these problems, polymer materials and the related fabrication technologies have emerged as a possible alternative to silicon-based devices, and great effort has been spent on finding innovative all-polymer solutions [3]. However, silicon possesses excellent optical, mechanical, and thermal properties that make it still preferred among other materials, especially by considering the well-established micro-opto-electro-mechanical systems (MOEMS) processes available to manufacture complex optical devices. For these reasons, innovative hybrid approaches have been recently proposed that make use of polymer for the realization of hybrid platforms [20–23]. By using these approaches, the microfluidic parts to manipulate liquid samples, comprising the fluidic inlet and outlet and the channels for delivering the sample, can be easily and cost-effectively fabricated in a polymer substrate. In particular, poly(dimethysiloxane) (PDMS) is one of the most widely used polymer materials in microfluidics due to its optical and chemical properties. PDMS is optically transparent in the visible/UV region and is non-toxic to proteins and cells. Moreover, PDMS-based devices can be manufactured by using simple and cost-effective fabrication processes like soft lithography [24].

Recently a hybrid polymer–silicon optofluidic anti-resonant reflecting optical waveguide (h-ARROW) has been proposed and tested [25], offering the prospective of combining silicon and polymer technologies into a compact hybrid platform.

In this paper we propose a hybrid approach for assembling an optofluidic chip for optical sensing of liquids. In our proposed h-ARROW platform, the microfluidic system has been fully realized with polymer using a modular approach while the optical part has been realized developing a polymer-silicon hybrid solution. In a very recent work of Parks et al. [26] the microfluidic processing system of an ARROW-based optofluidic chip was created in a PDMS layer. The fluidic and the optical chip were then integrated as two separate entities, making it possible to easily replace the fluidic processing layer. The approach presented here is different, as hybrid integration was also implemented for the fabrication of the optical element.

In the proposed device, a multimodal liquid core hybrid PDMS-silicon ARROW (h-ARROW) used for sample flowing and sensing was integrated with solid core hybrid PDMS-ARROW (solid h-ARROW) in a self-aligned optical layout. A first platform prototype with integrated a passive micro-mixer has been tested for fluorescence measurements.

2. Optofluidic platform design

The proposed platform is sketched in Fig. 1. It is composed of a modular structure with different functionalities on the same chip toward a fully integrated optofluidic device—a

#194578 - $15.00 USD Received 24 Jul 2013; revised 9 Sep 2013; accepted 9 Oct 2013; published 9 Jan 2014

bottom part with optical functionalities consisting of an h-ARROW with an integrated solid-core h-ARROW (Silicon-part and layer *a*) and a top part entirely realized by a PDMS-layered structure with microfluidic functionalities (layer *b*). In particular, as a first prototype, a passive micro-mixer with a serpentine path has been fabricated in layer *b*.

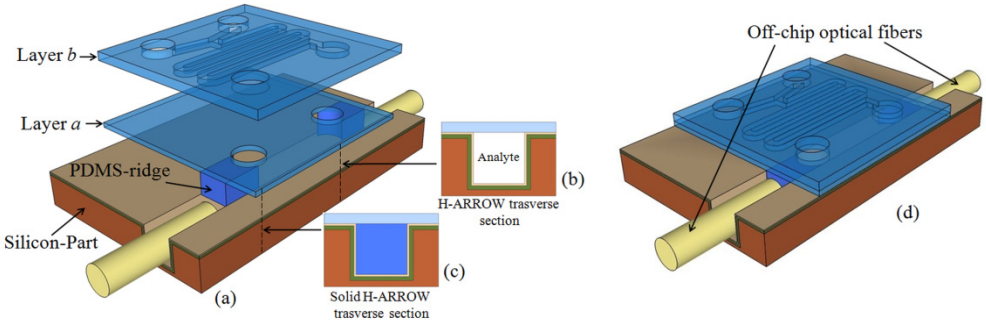

Fig. 1. (a) Exploded view drawing of the proposed hybrid ARROW optofluidic platform with transverse section of (b) liquid h-ARROW and (c) solid h-ARROW. (d) Schematic of the assembled device.

The optical guiding and sensing element of the proposed optofluidic platform consists of a liquid-core h-ARROW waveguide. Liquid-core ARROWs are widely recognized as a powerful tool in the field of optical sensing of liquid samples [14,16,27]; in these waveguides, the liquid sample and the probing light share the same path, enhancing the optical interaction and hence improving the sensitivity. The confinement in the core region is the result of anti-resonant reflection in the cladding layers. Low propagation losses in the visible wavelength range can be obtained with only two anti-resonant layers, properly designed to operate like a high-reflectivity Fabry–Perot mirror. Conventional full-silicon liquid ARROWs have been successfully applied in realizing integrated optical devices [28,29] and optofluidic chips for sensing applications [17].

In comparison to full silicon ARROW, in an h-ARROW the top silicon part is replaced by a single layer of PDMS [Fig. 1(b)] [25]. The great advantage of this configuration is the possibility of integrating the microfluidic system in the top polymer part, which can be easily fabricated using low-cost and fast fabrication approaches.

The coupling of light from off-chip optical fibers into the optofluidic channel is obtained via solid h-ARROWs integrated in the platform. Solid h-ARROWs differ from h-ARROWs only for core material, which is fabricated with high-refractive-index PDMS [Fig. 1(c)]. In particular, the optofluidic channel of a conventional silicon-based ARROW waveguide (silicon-part) was sealed with a PDMS layer (layer *a*) that constitutes the polymer part of the resulting h-ARROW waveguide. Two PDMS ridges with a suitable optical refractive index were fabricated on layer *a* in order to form the solid core of the fully integrated solid h-ARROW. A modified cure agent ratio composition was employed to fabricate the ridges, providing a higher optical refractive index to PDMS in particular by increasing the base agent portion results in an increase of the optical refractive index. The so-fabricated ridges were then inserted into the optofluidic ARROW channel to finally realize the proposed solid h-ARROW waveguides [Fig. 1(d)]. The light is confined in the solid core due to the ARROW guidance effect and total internal reflection effect, which takes place at the interface between the solid core and the top PDMS layer, thanks to the refractive index difference. This hybrid integration allows us to seal the liquid h-ARROW and to guide the light from/toward the exciting/collecting off-chip optical fibers. Moreover, off-chip fibers can be directly inserted into the end section of the optofluidic channel [Fig. 1(d)], resulting in a self-aligned optical layout where light from/to the exciting/collecting fibers propagates along the same optical axis of the h-ARROW and solid h-ARROW. Two holes were formed on layer *a* at the end of

#194578 - $15.00 USD Received 24 Jul 2013; revised 9 Sep 2013; accepted 9 Oct 2013; published 9 Jan 2014

both ridges to create the microfluidic connection between the bottom part of the platform and the upper PDMS layer (layer *b*).

As it can be seen from the platform sketch, the microfluidic system is stacked in the vertical direction, allowing us to superimpose additional PDMS layers with different microfluidic components. This modular approach allows the assembly of as many microfluidic layers as desired in order to achieve the highest possible flexibility and modularity of the platform without changing the more costly silicon part. Layering soft polymers is particularly advantageous, as good and conformal contact between surfaces is easily achieved at low pressure, thus eliminating thermal and mechanical stress that often occurs when layering hard materials. Moreover, the capability of temporary bonding to several materials makes PDMS very attractive for prototype and device development.

3. Hybrid waveguide fabrication and characterization

Due to the hybrid nature of the proposed chip, it was fabricated by a step-by-step hybrid fabrication process where the silicon-based part was fabricated using a bulk micromachining process and the polymer-based part by soft lithography.

3.1 Silicon-based ARROW fabrication

The fabrication steps of the silicon part of the platform are listed below. A photolithographic process and reactive dry etching were employed to define the core channel (depth of 150 μm and width of 130 μm). Two dielectric layers of silicon nitride (first cladding, refractive index n_1=2.01) and silicon dioxide (second cladding, n_2=1.47) were then deposited by plasma-enhanced chemical vapor deposition (PECVD) at a temperature of 450°C. The waveguide was designed to minimize the propagation loss for a water-filled core (n_c=1.33) at a wavelength of λ=670 nm. Accordingly, cladding thicknesses of d_1=334 nm (Si_3N_4) and d_2=270 nm (SiO_2) were chosen following the anti-resonant condition [25] at λ=670 nm. The core dimension permits a simple optical coupling by the insertion of optical fibers (125 μm cladding diameter) directly inside the core of the hollow waveguide [Fig. 1(a)].

3.2 H-ARROW with integrated solid h-ARROW fabrication

The fabrication of a solid-core h-ARROW starts with the fabrication of a PDMS ridge as shown in Fig. 2(a).

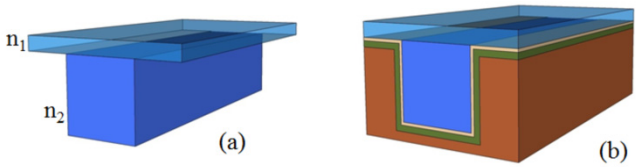

Fig. 2. (a) PDMS ridge, (b) soli-core h-ARROW.

In Figs. 3(a)–(e) the process steps necessary for the fabrication of the waveguides are schematized. A poly(methyl methacrylate) (PMMA) master was fabricated with a computer numerical control (CNC) micro-milling machine. PMMA is widely used as mold material due to its good machinability. Two grooves (130 μm wide and 150 μm deep) were machined in the substrate with a 127±12.7 μm end mill [Fig. 3(a)]. Due to the uncertainty, the end mill dimensions were measured before starting the process. At the end of the fabrication process, the dimensions of the grooves and of PDMS ridges were measured with an optical profilometer before being inserted in the silicon optofluidic channel. The groove size was chosen to match the ARROW core dimensions. The distance between the groove edges was set to d_1=7 mm. A thin PDMS layer (thickness of t~1 mm) was prepared by casting and curing PDMS (PDMS prepolymer was mixed with the curing agent in a weight ratio of 10:1)

#194578 - $15.00 USD Received 24 Jul 2013; revised 9 Sep 2013; accepted 9 Oct 2013; published 9 Jan 2014

between two PMMA slides in order to obtain a flat PDMS surface on both sides [Fig. 3(b)]. Two holes of 300 μm of diameter (A and B) centered at a distance of d_2=6.8 mm were created on layer *a*.

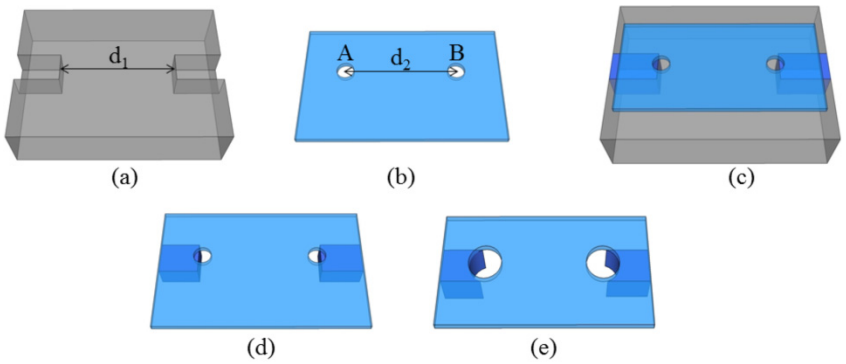

Fig. 3. (a) PMMA substrate with milled grooves; (b) thin PDMS layer with holes punched; (c) PMMA substrate with holed PDMS layer; (d) PDMS layer *a* after curing process; (e) layer *a* at the end of process.

After that, the layer was placed on the PMMA master by using a micrometer translation stage in order to obtain the proper alignment between the two parts. Particular attention was addressed to avoid the formation of air bubbles in between the two parts. As is shown in Fig. 3(c) the hole area was set to slightly overlap with the grooves; this arrangement gave rise to two open-ended grooves. PDMS pre-polymer was then mixed with its curing agent in a weight ratio of 2.5:1. The PDMS refractive index was measured with an Abbe refractometer, obtaining n_1=1.4105 and $n_{2=}$1.4115 for weight ratios 10:1 and 2.5:1, respectively [Fig. 2(a)]. The open-ended grooves were filled by the pre-cured elastomer by capillary effect until the holes were reached [Fig. 3(c)]. Once the grooves were completely filled, two needles were used to seal the holes in order to stop the pre-polymer flow. A curing process of the sample was performed at a temperature of T=60°C for 2 hours. During the heated curing process, the PDMS pre-polymer filling the grooves adhered to the top PDMS layer to form the ridge structures. The cured layer was gently removed from the PMMA substrate at the end of the process [Fig. 3(d)] and holes of 350μm in diameter centered with A and B were then punched onto the layer [Fig. 3(e)]. The layer with the PDMS ridges was lowered onto the silicon part by using a translation and rotation stage and a CCD camera to control the alignment. The optical transparency of PDMS allows checking the goodness of the adhesion and the absence of disturbing air bubbles between the two parts. Figure 4 shows a picture of the device as composed of a silicon part with layer *a* only superimposed. In the picture is also highlighted how the lack of adhesion due to the presence of unwanted air bubbles was clearly evident during the alignment procedure. The length of the PDMS ridges in the final device was about 10 mm. This length was chosen as a good compromise between the ability to align and seal the optofluidic channel. Longer ridge sections often led to a time consuming processing step to assure perfect alignment. On the other hand, shorter sections exhibited reduced propagation losses and made the alignment easier but at the expense of long-term leakage stability. Good adhesion was obtained and no leakage of liquid from the channel ends was observed with a flow rate ratio of up to 2 ml/hr.

#194578 - $15.00 USD Received 24 Jul 2013; revised 9 Sep 2013; accepted 9 Oct 2013; published 9 Jan 2014

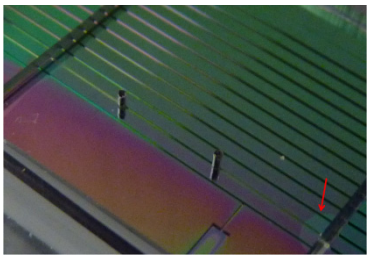

Fig. 4. Picture of the device during fabrication. Highlighted in the picture is the lack of adhesion due to the presence of unwanted air bubbles.

For the optical characterization, a 2 cm long solid-core h-ARROW with flat end facets was used [Fig. 2(b)]. The light-guiding effect was demonstrated by capturing the image of the field profile transmitted from the waveguide at λ=670 nm. The light was coupled with an optical fiber (105 μm core diameter). The transmitted intensity was imaged through a microscope objective on a CCD camera. The recorded image is shown in Fig. 5(a).

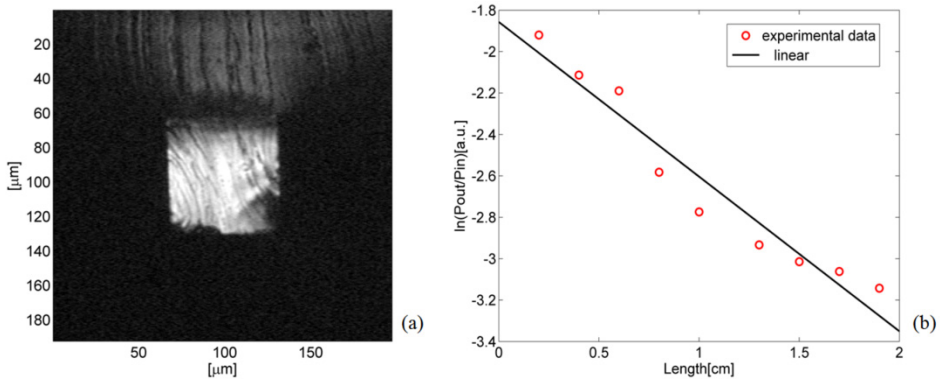

Fig. 5. (a) CCD captured output intensity distribution. (b) Transmitted intensity versus waveguide length (symbol: experiment; line: exponential fit).

Attenuation losses were measured by using the cut-back method on a 2 cm long solid h-ARROW. A full-polymer PDMS-waveguide sample [Fig. 2(a)] was cleaved into successively shorter waveguides and inserted in the ARROW channel. The measurement was performed on each resulting sample with a laser diode at λ=670 nm coupled into a multimodal optical fiber (105 μm core diameter). The transmitted power was collected using an optical fiber (105 μm core diameter) and sent to an optical power meter. By fitting the experimental data by means of mono-exponential decay, we found an attenuation loss of 3.25 dB/cm [Fig. 5(b)]. Total fiber-to-waveguide insertion losses for both sides of the waveguide of 8.06 dB were estimated from the y-intercept of the linear fit. This relatively high value can be explained by taking into account the core size difference and the modal mismatch that decreased the optical coupling. The measured propagation loss in the liquid section was 7.6 dB/cm. This result was reasonable as compared to results reported in [30] by considering that in an h-ARROW it was expected that there would be a slight increase of the loss due to the hybrid configuration [25]. Substantial yield improvements of propagation loss in an ARROW waveguide can be achieved by adding two or more anti-resonant layers [25]. To simplify the process step of the silicon part, only two cladding layers were used for light confinement in the fabricated liquid h-ARROW.

#194578 - $15.00 USD Received 24 Jul 2013; revised 9 Sep 2013; accepted 9 Oct 2013; published 9 Jan 2014

4. Microfluidic layer fabrication

The upper part of the platform (layer *b*) consists of a true PDMS layer where microfluidic devices can be integrated using a soft lithography process. In the proposed prototype, a passive micro-mixer was employed to create solutions at different fluorophore concentrations. In this device the mixing process is governed by slow diffusion at the interface of two co-flowing liquids under the laminar flow. For this reason, in order to have a long path for efficient mixing, a serpentine-based micro-mixer design was used. The total length of the serpentine was estimated by taking into account that the time the particles or molecules take to diffuse across the entire channel is given by $\tau \sim w^2/D$, where *w* is the width of the channel and D is the diffusion coefficient of the considered species. The distance traveled along the channel by the stripe during this time interval will be $L \sim U_0\tau$, where $U_0=Q/w^2$ is the stripe velocity and Q is the flow rate. Hence, the minimum length of the serpentine for efficient mixing can be calculated as L=Q/D [31].

A PDMS-based microfluidic mixer has been fabricated by replica-molding of a microstructured PMMA stamp from a PDMS master, following the procedure reported in [32]. First, the micro-mixer was fabricated by the direct milling of a PMMA substrate [Fig. 6(a)], followed by the molding of the PDMS with micro-fabricated PMMA as the master [Fig. 6(b)]. The replica of the microstructured PMMA stamp was finally obtained by molding the PDMS with the PDMS master [Fig. 6 (c)].

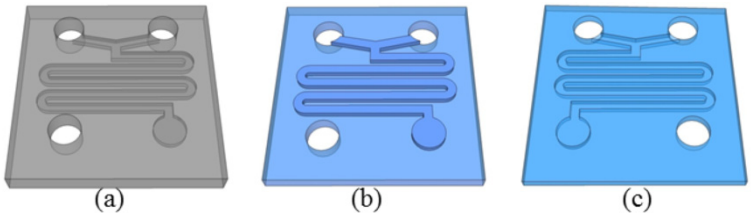

Fig. 6. (a) Micro-mixer fabricated in the PMMA master by direct milling. (b) PDMS mold of PMMA master. (c) PDMS replica of PMMA master.

This fabrication technique has been preferred over the fabrication of a PMMA master directly by a milling machine for several reasons: since only the microfluidic channels were milled in PMMA, the time required for machining was strongly reduced and hence the cost; moreover, the PDMS-adhering contact area is very flat, being molded from a non-machined PMMA area.

The diffusion coefficient of Cy5 dye molecules in water is $D \sim 3.6\times10^{-6}$ cm^2/s. The microfluidic channel dimension was set to 200 μm×200 μm. Hence, for a flow rate ratio up to Q=0.5 ml/hr, the required length of the serpentine for complete mixing was L~Q/D=38.5 cm. The length of the fabricated mixing section was 42 cm.

In order to test the flexibility of the process for rapid prototyping assembly, the various layers were reversibly joined. PDMS makes reversible Van der Waals contact against PDMS and also against Si_3N_4, which was strong enough to preserve a good contact between the parts during our measurements. We did not observe any liquid leakage from the waveguide ends for a flow rate up to 2ml/hr, indicating that a leak-tight seal was formed. More robustness could obtained by using external clamps that permit the benefit of reversible sealing. Alternatively, only layer *a* (Fig. 1) could be permanently bonded to the silicon part, leaving the microfluidic layer free to be replaced.

5. Application: fluorescence measurements

The potential of the proposed chip for sensing applications was demonstrated by fluorescence measurements on a liquid sample flowing in the h-ARROW optofluidic channel. Fluorescence is one of the most widely used optical methods for molecular sensing in microfluidic systems

#194578 - $15.00 USD Received 24 Jul 2013; revised 9 Sep 2013; accepted 9 Oct 2013; published 9 Jan 2014

due to well-established and highly selective fluorescent labeling techniques. Water solutions of Cy5 dye in a concentration ranging from 2.5×10^{-10}M and 7.8×10^{-6} M were used. Syringe pumps were used to drive the flow of fluids in the channels. Syringe needles with an outer diameter of 500 μm and an inner diameter of 260 μm were inserted into holes bored in the PDMS. To introduce and recover liquids from micro-channels, polytetrafluoroethylene (PTFE) tubing conforming to syringe needles was used. The optofluidic chip comprises two inlet ports connected to the mixer (D and C) and an outlet port (A) connected to the h-ARROW channel for recovering liquids [Fig. 7(a)]. Water solutions containing Cy5 dye and pure water were injected into inlets D and C, respectively. The desired mixing was obtained by controlling the flow rate ratio between the two co-flowing streams. The measured concentration range could not be explored as a whole by varying the volume ratio between the channels in a single step. For example, the concentration values of [10^{-9}M 5×10^{-10}M 2.5×10^{-10}M] were explored by injecting in inlet D a concentration of $c_0=1.5\times10^{-10}$M and by varying the flow rate ratio between inlet C (pure water) and inlet D in the range of [0.36 2.76 12.8].

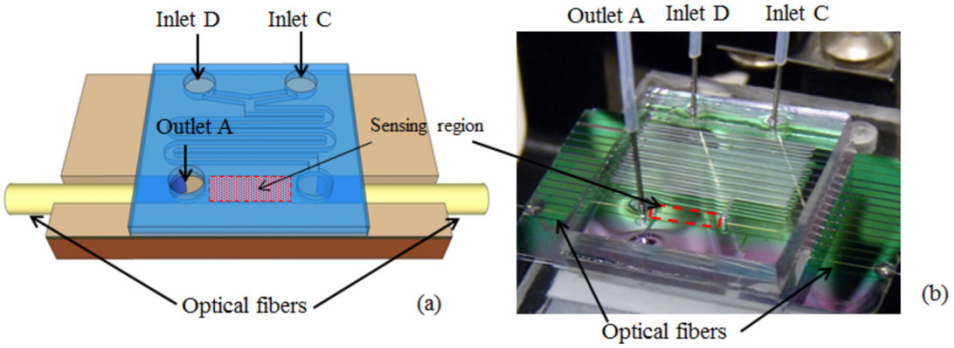

Fig. 7. (a) Schematic and (b) photograph of the chip.

A collimated laser diode (1 mW) emitting at λ=635 nm was used as exciting source in an orthogonal excitation/collection optical scheme in order to reduce the pump contribution to the detected optical signal. A spectroscopy system (Andor Technology) comprised of a spectrograph (Shamrock 303i) integrated with a CCD camera (Newton 971) was used to detect the fluorescence signal. The sensing volume of about 130 nl was illuminated by using a cylindrical lens in the excitation path. A translation stage was used to accurately position the device to uniformly illuminate the sensing region. The entire region was illuminated (instead of just a spot near the collection end) in order to have larger sensing volume due to the quite high h-ARROW-to-fiber insertion losses. A multimode optical fiber (105/125 μm core/cladding diameter) was inserted in the h-ARROW channel to collect the fluorescence signal. Due to the elastomeric properties of PDMS that make it very easily deformable, the optical fiber tip was gently pressed against the solid h-ARROW facet in order to optimize the optical coupling.

As shown in Fig. 7(a), the length of the fabricated ARROW optofluidic channel can be chosen opportunely in order to allow the insertion of two optical fibers that can be used to provide light excitation and collection along the same propagation axis. In the proposed fluorescence experiment, an excitation from the top has been employed to reduce the pump contribution to the fluorescence detected signal. Hence, during the experiment, only one of the two available fibers has been used to collect the signal.

The fluorescence intensity has been evaluated as the integral of the measured optical spectrum between 646 nm and 750 nm. Each spectrum is the average value of 50 samples acquired using an integration time of 1s. The experimental results and corresponding limit of

#194578 - $15.00 USD Received 24 Jul 2013; revised 9 Sep 2013; accepted 9 Oct 2013; published 9 Jan 2014

detection (LOD) are shown in Fig. 8. The LOD gives the minimum detectable concentration of Cy5. It is defined as the intercept between the fluorescence fit curve with a horizontal line (black line) whose value is given by the sum of the noise intensity (i.e., calculated from the spectrum of pure water) and three times its standard deviation. From measurements we found an LOD of 2.5 nM. The reported sensitivity is quite high as compared with other compact devices for fluorescence detection [33–36]. In the proposed device the sensitivity is substantially limited by the fluorescence collection efficiency, in particular by the optical losses of the liquid and solid section, and, mainly, by the fiber-to solid h-ARROW insertion losses. Further developments could be made in the soft-lithography fabrication process with the aim of reducing the residual surface roughness of the solid h-ARROW end facet and hence improve the coupling efficiency.

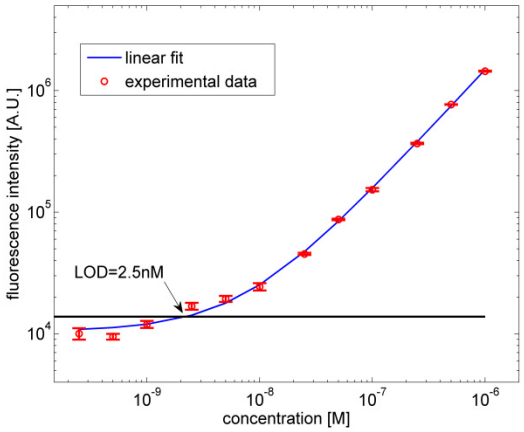

Fig. 8. Fluorescence intensity measurements versus concentration of Cy5 in water.

6. Conclusion

An optofluidic platform with a hybrid polymer–silicon modular approach has been proposed. Optofluidic hybrid ARROW waveguides have been designed and fabricated with monolithic integrated solid-core waveguides for a high level of integration and simplified optical coupling. The core of the solid h-ARROW has been manufactured with low-cost materials and a fast fabrication process. From the optical characterization, optical losses of 3.25 dB/cm and total fiber-to-waveguide insertion losses for both sides of the waveguide of 8.06 dB have been found.

A first prototype of the platform has been presented with an integrated micro-mixer as part of the microfluidic system. The device has been applied for fluorescence measurements to test the sensing performance. A good detection limit of 2.5 nM has been obtained, showing a promising capability for further performance improvements. In particular, the measured propagation losses indicate the need for further improvement of the fabrication process involved in the polymer-based optical sections.

We believe that the proposed modular approach represents a first step toward a truly hybrid optofluidic chip, offering the promise of more rapid prototyping and allowing greater adaptability, as the microfluidic part can be easily replaced, rearranged, and adapted to different detection schemes.

Acknowledgments

The research leading to these results has received the financial support of the Italian Minister of University and Research (MIUR) Futuro in Ricerca (FIRB) programme under grant 151J12000310001 (SENS4BIO).